MEDICAL SCIENCE MONITOR

LAB/IN VITRO RESEARCH

e-ISSN 1643-3750
© Med Sci Monit, 2018; 24: 2339-2349
DOI: 10.12659/MSM.909144

Received: 2018.01.24
Accepted: 2018.03.29
Published: 2018.04.18

Propofol Inhibits HeLa Cells by Impairing Autophagic Flux via AMP-Activated Protein Kinase (AMPK) Activation and Endoplasmic Reticulum Stress Regulated by Calcium

Authors' Contribution:
Study Design A
Data Collection B
Statistical Analysis C
Data Interpretation D
Manuscript Preparation E
Literature Search F
Funds Collection G

ABEF Xi Chen
CD Kai Li
AG Guoqing Zhao

Department of Anesthesiology, China-Japan Union Hospital of Jilin University, Changchun, Jilin, P.R. China

Corresponding Author: Guoqing Zhao, e-mail: guoqingzhao1965@163.com
Source of support: This research was funded by the National Natural Science Foundation of China (81502516) and the Social Development Project of Jilin Province (3D516P883430) to Guoqing Zhao

Background: Propofol has antitumor effects against various cancers. However, the mechanism of action of propofol in HeLa human cervical cancer cells has not been elucidated.

Material/Methods: We treated HeLa human cervical cancer cells with different concentrations of propofol. Cell viability was evaluated with Cell Counting Kit-8 and apoptosis was analyzed by annexin V-fluorescein isothiocyanate and propidium iodide staining and flow cytometry. Autophagosome formation was evaluated based on microtubule-associated protein light chain (LC)3 conversion and light chain 3 puncta formation. Autophagosome clearance was assessed according to p62 protein level and autolysosome generation.

Results: We found that propofol decreased cell viability and increased autophagosome generation in HeLa cells. Autophagosome formation was evaluated based on LC3 conversion and LC3 puncta formation. Autophagosome clearance was assessed according to p62 protein level. The AMPK/mTOR signaling pathway was found to be activated in propofol-induced autophagosome accumulation. Fluorescence analysis using LysoTracker dye revealed that propofol blocked autophagosome–lysosome fusion. Administration of rapamycin increased autophagosome clearance in propofol-treated HeLa cells. Additionally, propofol induced endoplasmic reticulum (ER) stress and disrupted intracellular Ca^{2+} balance, thereby enhancing autophagosome accumulation. Suppressing ER stress by treatment with tauroursodeoxycholic acid (TUDCA) enhanced these effects, suggesting that the cytotoxicity of propofol is related to induction of ER stress.

Conclusions: This study is the first to provide evidence that propofol-mediated autophagy regulation is an underlying part of the mechanism by which propofol regulates HeLa cells progression.

MeSH Keywords: Autophagy • Propofol • Uterine Cervical Neoplasms

Full-text PDF: https://www.medscimonit.com/abstract/index/idArt/909144

Indexed in: [Current Contents/Clinical Medicine] [SCI Expanded] [ISI Alerting System] [ISI Journals Master List] [Index Medicus/MEDLINE] [EMBASE/Excerpta Medica] [Chemical Abstracts/CAS]

Background

Propofol (2, 6-diisopropylphenol) is widely used for the induction and maintenance of anesthesia [1]. Recent studies suggest that propofol also exerts antitumor effects [2]. Propofol was found to suppress HeLa human cervical cancer cell invasion [3]. In addition, propofol induces autophagy in some organs [4], which has been shown to potentiate the antitumor efficacy of some drugs [5].

Autophagy is a dynamic process comprising 2 consecutive stages. The first step is autophagosome formation. The second step is autophagosome clearance, which involves autolysosome formation via autophagosome–lysosome fusion [6,7]. Inhibiting autophagic flux can sensitize cells to stimulus-induced damage and cell death [7–10]. Mammalian target of rapamycin (mTOR) is described as a key homeostatic regulator of cell growth, proliferation, and survival as well as metabolism by upregulating protein synthesis and inhibiting excessive autophagy. Inhibition of mTOR leads to induction of autophagy. Adenine nucleotide (AMP)-activated protein kinase (AMPK) activity is generally antagonistic toward mTOR function. Recent evidence suggests that endoplasmic reticulum (ER) stress is a potent inducer of autophagy [11]. The ER is an organelle that regulates protein secretion and maintains intracellular Ca^{2+} concentration [12,13]. Indeed, ER stress results in the perturbation of cellular Ca^{2+} homeostasis and cell death. Propofol significantly increases peak and integrated Ca^{2+} responses [14]; however, it is unclear whether its anticancer effects involve modulation of ER stress and Ca^{2+} homeostasis.

We addressed these questions in the present study by treating HeLa cells with propofol and evaluating the effects on cell proliferation and autophagy as well as the underlying mechanisms. Our results demonstrate that impairment of autophagic flux is an underlying part of the mechanism by which propofol regulates cancer progression.

Material and Methods

Cell culture, drug treatment, and reagents

HeLa cells were obtained from the Institute of Science Center. Cells were grown in Dulbecco's modified Eagle's medium (DMEM) supplemented with 10% fetal bovine serum (FBS) and penicillin-streptomycin (all from Biological Industries, Cromwell, CT, USA) at 37°C in a humidified incubator with 5% CO_2. Polyclonal antibody against LC3-I/II (Sigma-Aldrich, St. Louis, MO, USA) and monoclonal antibodies against C/EBP-homologous protein (CHOP), LC3, p62, lysosomal-associated membrane protein -1 (LAMP-1) AMPK, phosphorylated (p-) AMPK, mTOR, p-mTOR, binding immunoglobulin protein (Bip), glyceraldehyde 3-phosphate dehydrogenase (GAPDH), inositol-requiring protein-1α (IRE-1α), and p-IRE-1α (all from Cell Signaling Technology, Danvers, MA, USA) were used at 1: 1000 dilution. Goat anti-mouse and -rabbit IgG secondary antibodies were purchased from Li-Cor (NE, USA). Magic Red Cathepsin B Assay kit was purchased from ImmunoChemistry (Bloomington, MN, USA). All the experiments were performed with 400 μM propofol treatment for 3 h unless stated otherwise. Propofol (Sigma-Aldrich; D126608) was prepared in dimethylsulfoxide and diluted in DMEM. Rapamycin and chloroquine (CQ) were purchased from Selleck Chemicals (Houston, TX, USA). In some experiments, cells were co-treated with 1 mM TUDCA (Aladdin, Shanghai, China; S101371) or 10 μM CQ. In others, cells were pre-treated with 10 mM rapamycin for 30 min.

Cell viability

Cell suspensions (7000 cells/100 μl) were seeded in a 96-well plate, then exposed to propofol for 3 h or 24 h. The cells were washed with DMEM and then incubated with 10 μl of CCK-8 solution for 1–2 h, after which the absorbance was measured at 450 nm.

Apoptosis

Apoptotic cells were quantified with an annexin V and PI (propidium iodide) detection kit and by flow cytometry analysis. Briefly, cells were treated with 400 or 800 μM propofol for 3 h, washed twice with PBS, resuspended in 1 ml of binding buffer, stained for 15 min at room temperature with annexin V and PI, and sorted on a FACS Calibur instrument with CellQuest software.

Western blot analysis

Samples (50 μg) were separated for 3 h at 80 V by sodium dodecyl sulfate polyacrylamide gel electrophoresis on 8–15% gels and transferred for 2 h at 100 V to a polyvinylidene difluoride membrane that was then blocked in 4% skim milk for 1 h and probed overnight at 4°C with primary antibodies. After three 5-min washes, the membrane was incubated for 2 h at room temperature with secondary antibodies. Protein bands were visualized with an Odyssey Image Analyzer 3.0 (Li-Cor).

Examination of GFP-LC3 punctae

GFP-LC3 punctae were observed on an Operetta high-throughput optical imager (Perkin-Elmer, Waltham, MA, USA) and analyzed with the integrated Columbus image data storage and analysis system (Perkin-Elmer). The number of LC3 punctae was counted in more than 60 randomly selected cells from 1 batch of 4–5 independent experiments [6,7].

Indexed in: [Current Contents/Clinical Medicine] [SCI Expanded] [ISI Alerting System] [ISI Journals Master List] [Index Medicus/MEDLINE] [EMBASE/Excerpta Medica] [Chemical Abstracts/CAS]

Evaluation of lysosomal pH

Lysosomal pH was evaluated using the LysoSensor Yellow/Blue DND-160 reagent, which shows a pH-dependent increase in fluorescence intensity upon acidification [6,7,15]. Cells were stimulated with propofol (400 μM) or CQ (10 μM) for 3 h, then incubated with 5 μM LysoSensor reagent for 1 h. Fluorescence intensity was examined with the Operetta high-throughput optical imager and analyzed with the integrated Columbus image data storage and analysis system.

Examination of autophagosome–lysosome fusion

The cells were incubated with LysoTracker Red DND-99 (75 nM), which is an acidic pH marker for lysosomes, for 30 min to visualize lysosomes [16–18]. The co-localization of GFP-LC3 punctae and LysoTracker was examined with the Operetta high-throughput optical imager and analyzed with the integrated Columbus image data storage and analysis system. The rate of autophagosome–lysosome fusion was calculated as the percentage of autolysosomes relative to autophagosomes.

Cathepsin B activity assay

Cathepsin B activity was measured using a Magic Red Cathepsin B assay kit (Bio-Rad) according to the manufacturer's instructions. Images were captured with the integrated Columbus image data storage and analysis system.

Rhod-2AM staining

Cells were incubated at 37°C for 3 h with or without 400 μM propofol, TUDCA, or both. Cells were simultaneously stained with 3 μM Rhod-2AM ester (Biotium, Fremont, CA, USA, 50023) to follow changes in fluorescence intensity of Ca^{2+}. Finally, cells were imaged at 1 h, 2 h, and 3 h on an Operetta high-throughput optical imager and analyzed with the integrated Columbus image data storage and analysis system.

Statistical analysis

There was no priori power analysis conducted prior to the study. The sample size was in accordance with previous similar studies [19,20]. There were no missing data in this study. Data are presented as the mean ±SD. Groups were compared with the two-tailed unpaired t test or by one-way analysis of variance followed by Tukey's post hoc test, as appropriate, using SPSS v. 16.0 software (SPSS Inc., Chicago, IL, USA). Statistical significance was set at $p<0.05$.

Results

Propofol inhibits HeLa cell growth

HeLa cells were treated with different concentrations of propofol. Cell viability and apoptosis were examined. Treatment with propofol at concentrations of 0, 50, 100, and 200 μM had no effect on cell survival (Figure 1A). However, exposure to 400, 800, and 1600 μM propofol for 24 h significantly reduced cell viability in a concentration-dependent manner (Figure 1B). Propofol treatment for 3 h had no effect on the viability of HeLa cells (Figure 1C). However, exposure to 800 μM propofol for 24 h increased cell apoptosis (Figure 1D). Our results indicated that 400 μM propofol decreased cell viability, but did not induce apoptosis, in HeLa cells. Our research focused on whether propofol induces autophagy and on the effect of autophagy in the antitumor effect of propofol. This concentration was used in all subsequent experiments unless stated otherwise.

Propofol interferes with autophagosome–lysosome fusion

We examined the formation of green fluorescent protein (GFP)-LC3 puncta as a marker of autophagosomes [7]. The number of GFP-LC3 puncta was higher in cells exposed to propofol than in untreated control cells (Figure 2A). We next examined LC3 conversion, which is also a marker of autophagosome formation, by Western blot analysis [6,7,21]. The LC3-II/GAPDH ratio was increased in a concentration-dependent manner in propofol-treated cells relative to controls (Figure 2B). p62 is a marker of autophagosome degradation. Figure 2B shows that propofol treatment significantly increased the p62 protein level compared with that in the untreated controls. To clarify this point, a flux experiment was performed using CQ, a weakly basic amine that inhibits the late stage of autophagy by increasing lysosomal pH and inhibiting lysosomal enzymes post-sequestration to prevent autophagosome degradation. LC3-II levels induced by propofol in association with CQ were significantly higher than those observed with propofol or CQ alone (Figure 2C). The possibility that autophagosome accumulation might occur in the present experimental setting cannot be disregarded.

The propofol-induced accumulation of autophagosomes could be due to either an increase in autophagosome generation caused by activation of early autophagy or blockade of autolysosome clearance caused by inhibition of late autophagy. We next investigated whether propofol impaired autophagosome clearance. HeLa cells treated with CQ served as a positive control for lysosomal pH neutralization. Fluorescence was unchanged in the presence of 400 μM propofol but was diminished by CQ relative to that in untreated control cells (Figure 2D). Cathepsin B is a proteinase contained in lysosomes. Cathepsin B activity was 40.4% higher in cells treated with propofol than in the control groups (Figure 2E). Lysosomal

Indexed in: [Current Contents/Clinical Medicine] [SCI Expanded] [ISI Alerting System] [ISI Journals Master List] [Index Medicus/MEDLINE] [EMBASE/Excerpta Medica] [Chemical Abstracts/CAS]

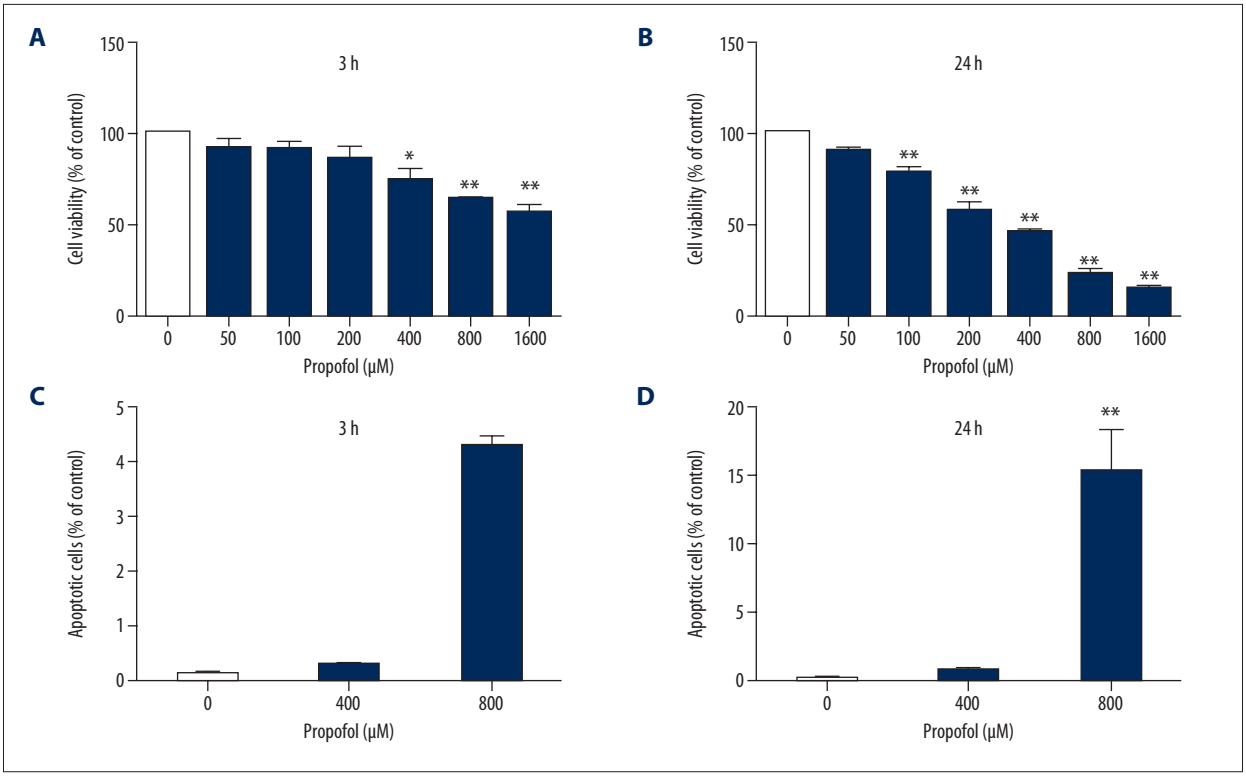

Figure 1. Propofol inhibits HeLa cell growth. Propofol inhibits HeLa cell growth. (**A, B**) HeLa cells were incubated with 0, 50, 100, 200, 400, 800, or 1600 μM propofol for 3 h (**A**) or 24 h (**B**), and cell viability was determined with the CCK-8 assay. (**C, D**) Apoptosis was detected by annexin V/PI staining and flow cytometry. Data are expressed as the mean ±S.D, n=3, * P<0.05, ** P<0.01 versus the control group. n=3 per group.

abundance is important for autophagosome clearance and was evaluated by examining the fluorescence of LysoTracker and the levels of LAMP-1 [17]. The intensity of red fluorescence of LysoTracker was 28.9% higher in propofol-treated as compared to untreated control cells (Figure 2F) indicating that lysosomal abundance and activity were not diminished by propofol treatment. Consistent with this observation, LAMP-1 levels were upregulated following exposure to propofol (Figure 2G). Thus, propofol-induced impairment of autophagosome clearance is unlikely to be caused by dysregulation of lysosomal abundance and activity. Then, we examined autolysosome formation. Autophagosomes were visualized as GFP-LC3 puncta (green fluorescence), whereas lysosomes were labeled with LysoTracker [18,22]. A yellow (green + red) fluorescence signal indicates normal autolysosome formation. Such signals were observed in the control group, whereas the colocalization rate of green and red fluorescence in cells treated with propofol was reduced by 54.0% (Figure 2H). These results demonstrate that propofol inhibits autolysosome formation by interfering with autophagosome–lysosome fusion. To determine whether autophagosome accumulation is involved in the antitumor effects of propofol in HeLa cells, we also observed that cell viability was decreased in the presence of CQ (Figure 2I). CQ potentiates the inhibitory effect of propofol on cell viability.

Propofol activates AMPK/mTOR signaling

Recently, several studies have suggested that the activation of AMPK promotes autophagosome formation in various cells; thus, we investigated whether propofol stimulates autophagosome generation by examining the activation of AMPK, which is known to stimulate this process [21,23]. mTOR prevents excessive autophagy [24] and is frequently dysregulated in human cancers [25]. Propofol treatment decreased mTOR phosphorylation in a concentration-dependent manner relative to control cells, whereas the opposite trend was observed for AMPK phosphorylation (Figure 3A). Pre-administration of rapamycin decreased cell viability (Figure 3C) and increased the LC3-II/GAPDH ratio as compared to cells treated with propofol alone (Figure 3B), whereas the p62 protein level was decreased. Similar trends were observed in cells treated with rapamycin alone. The colocalization rate of GFP-LC3 punctae and LysoTracker signal was also increased in the propofol group co-treated with rapamycin, as compared to the propofol-only group (Figure 3D). Therefore, propofol appears to be both an mTOR inhibitor and an AMPK activator. Propofol induces autophagy at least partly through the AMPK-mTOR signaling pathway.

Indexed in: [Current Contents/Clinical Medicine] [SCI Expanded] [ISI Alerting System] [ISI Journals Master List] [Index Medicus/MEDLINE] [EMBASE/Excerpta Medica] [Chemical Abstracts/CAS]

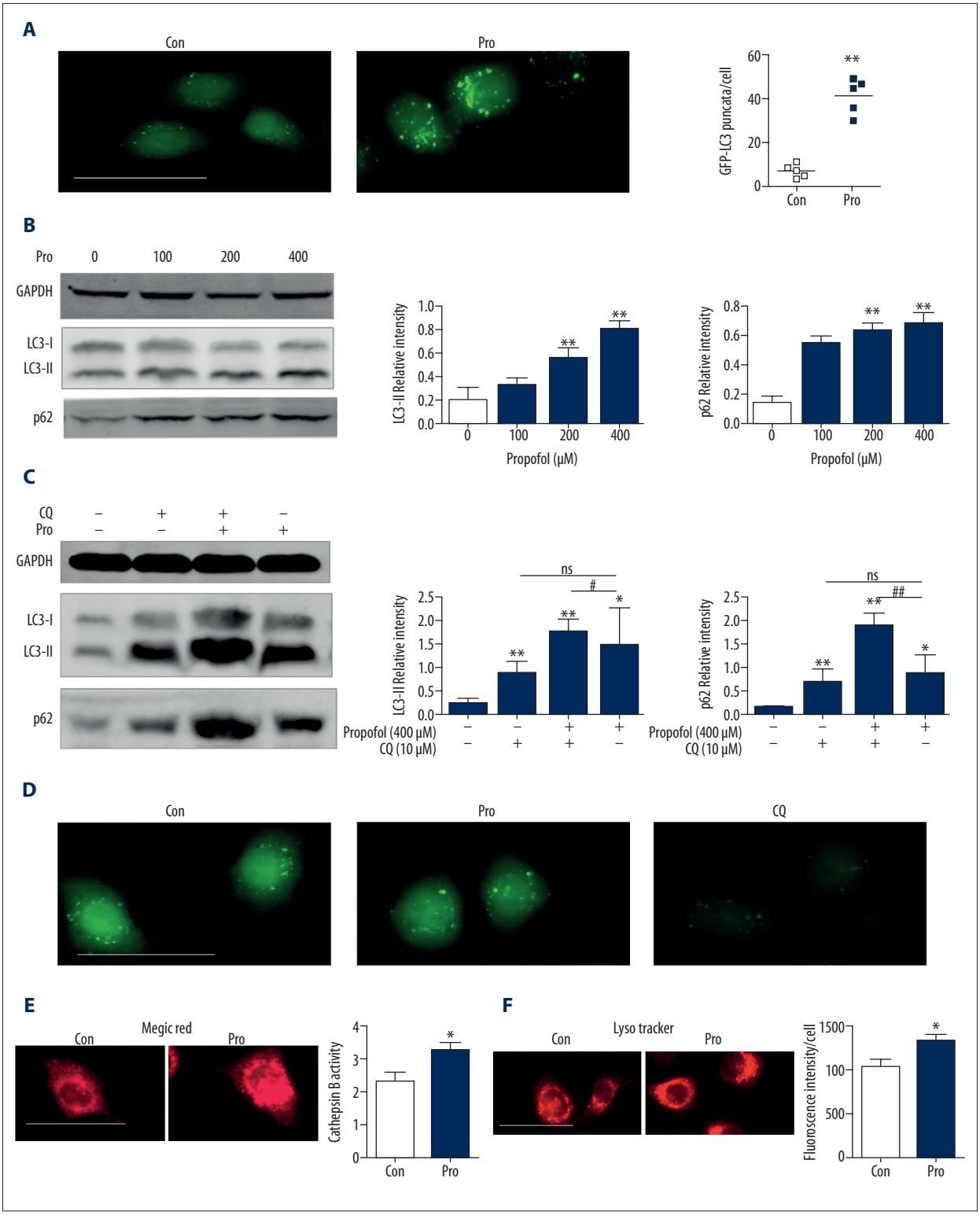

Indexed in: [Current Contents/Clinical Medicine] [SCI Expanded] [ISI Alerting System] [ISI Journals Master List] [Index Medicus/MEDLINE] [EMBASE/Excerpta Medica] [Chemical Abstracts/CAS]

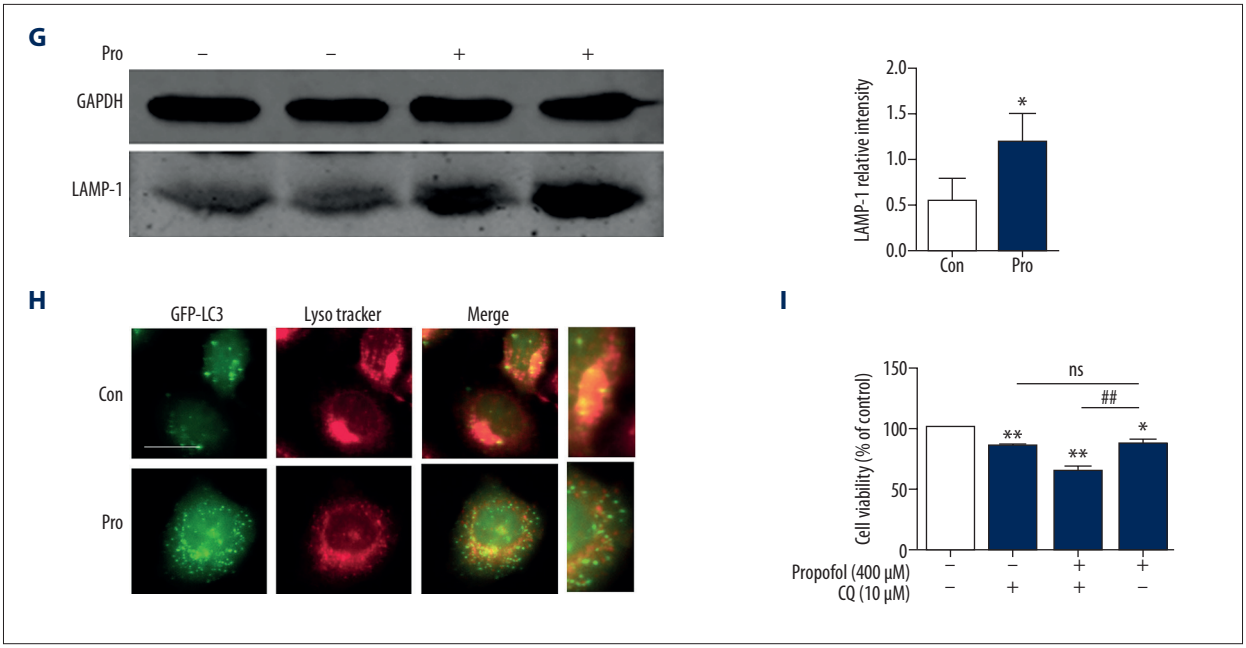

Figure 2. Propofol interferes with autophagosome–lysosome fusion. (**A**) HeLa cells stably expressing GFP-LC3 were exposed to propofol ([Pro] 400 μM) for 3 h. Untreated cells served as controls (Con). LC3 punctae were quantified. Representative images from 4 or 5 independent experiments are shown (scale bar=50 μm). (**B**) LC3 conversion and p62 levels in HeLa cells, as detected by western blot analysis. (**C**) HeLa cells were treated with propofol ([Pro] 400 μM) for 3 h, and untreated cells served as controls (Con). LC3 and p62 levels in propofol-treated HeLa cells with or without CQ (10 μM) treatment for 3 h. Propofol interferes with autophagosome–lysosome fusion. (**D**) To detect changes in lysosomal pH, cells were stained with LysoSensor and fluorescence was evaluated (scale bar=50 μm). Representative images from 3 independent experiments are shown. (**E**) Cathepsin B activity was evaluated with the Magic Red Cathepsin B Assay kit. Fluorescence images were acquired (scale bar=50 μm) and fluorescence intensity was quantified. (**F**) To detect autophagosome–lysosome fusion, cells were stained with LysoTracker. Fluorescence images were acquired (scale bar=50 μm) and fluorescence intensity was quantified. (**G**) Lysosomal-associated membrane protein 1 (LAMP-1) levels were evaluated by Western blot analysis, with GAPDH serving as a loading control. (**H**) HeLa cells stably expressing GFP-LC3 were stimulated with propofol ([Pro] 400 μM) for 3h; untreated cells served as the control (Con). Cells were stained with LysoTracker, and fluorescence was visualized (scale bar=20 μm). Higher-magnification views of the boxed areas are shown in the panels to the right. Representative images from 3 independent experiments are shown. (**I**) HeLa cells were co-incubated with 400 μM propofol with or without CQ (10 μM) for 3 h, and cell viability was evaluated with CCK-8. Data are expressed as the mean ±S.D, n=3, * $p<0.05$, compared with the control group; ** $p<0.01$, compared with the control group; # $p<0.05$, compared with the propofol group; ## $p<0.01$, compared with the propofol group.

ER stress plays a key role in propofol-induced autophagosome accumulation

To determine whether ER stress is involved in the effects of propofol on autophagy, HeLa cells were exposed to TUDCA, an inhibitor of ER stress. Treatment with TUDCA in the presence or absence of propofol suppressed the expression of ER stress and autophagy markers, as determined by Western blot analysis (Figure 4A). In particular, LC3-II, p62, Bip, and CHOP were upregulated and the ratio of p-IRE-1α to IRE-1α was increased upon exposure to propofol, and this effect was abrogated in the presence of TUDCA. Treatment with TUDCA with or without propofol decreased the number of LC3-positive puncta in GFP-LC3-expressing HeLa cells (Figure 4B) with a corresponding increase in cell viability (Figure 4C). Thus, propofol treatment increases autophagosome accumulation and exerts cytotoxic effects by stimulating the ER stress response in HeLa cells.

To determine whether ER stress is associated with Ca^{2+} homeostasis, we compared Ca^{2+} fluorescence between propofol-treated cells with or without TUDCA co-treatment. To quantify changes in cellular Ca^{2+}, cells were stained with Rhod-2AM, an indicator of intracellular Ca^{2+}. Fluorescence intensity was increased in cells treated with propofol (Figure 4D), and this effect was abolished in the presence of TUDCA. The fluorescence intensity increased more in the cells treated with propofol than in the control group at 1 h. The fluorescence intensity was higher in control cells and cells treated with propofol, with the propofol-treated cells showing a further increase at 2 h. Ca^{2+} homeostasis was disrupted by propofol, whereas the fluorescence intensity was lower in cells exposed to TUDCA

Indexed in: [Current Contents/Clinical Medicine] [SCI Expanded] [ISI Alerting System] [ISI Journals Master List] [Index Medicus/MEDLINE] [EMBASE/Excerpta Medica] [Chemical Abstracts/CAS]

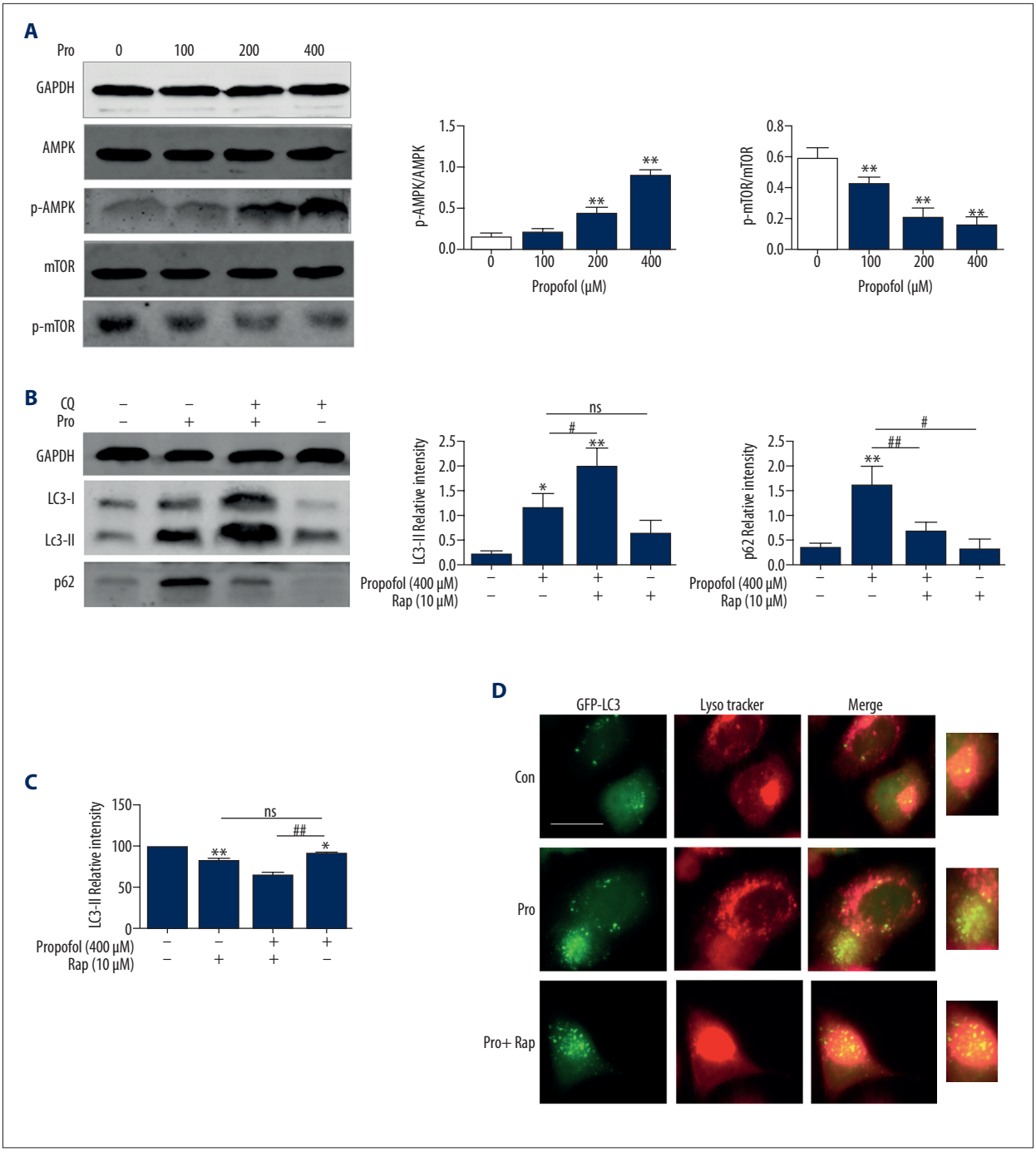

Figure 3. Propofol activates AMPK/mTOR signaling. (**A**) Hela cells treated with 100, 200, and 400 μM propofol for 3 h were analyzed by Western blot analysis for phosphorylated AMPK and mTOR. (**B**) HeLa cells were pre-incubated with 10 mM rapamycin for 30 min with or without 400 μM propofol for 3 h. LC3 conversion and p62 levels in HeLa cells, determined by Western blot analysis. (**C**) HeLa cells were pre-incubated with 10 mM rapamycin for 30 min with or without 400 μM propofol for 3 h, and cell viability was assessed with CCK-8. (**D**) HeLa cells were pre-incubated with 10 mM rapamycin for 30 min with or without 400 μM propofol for 3 h. Then, HeLa cells were stained with LysoTracker. Fluorescence was visualized and images were acquired (scale bar=20 μm). Higher-magnification images of the boxed areas are shown in the panels to the right. Representative images from 3 independent experiments are shown. Data are expressed as the mean ±S.D, n=3, * p<0.05, compared with the control group; ** p<0.01, compared with the control group; # p<0.05, compared with the propofol group; ## p<0.01, compared with the propofol group.

Indexed in: [Current Contents/Clinical Medicine] [SCI Expanded] [ISI Alerting System] [ISI Journals Master List] [Index Medicus/MEDLINE] [EMBASE/Excerpta Medica] [Chemical Abstracts/CAS]

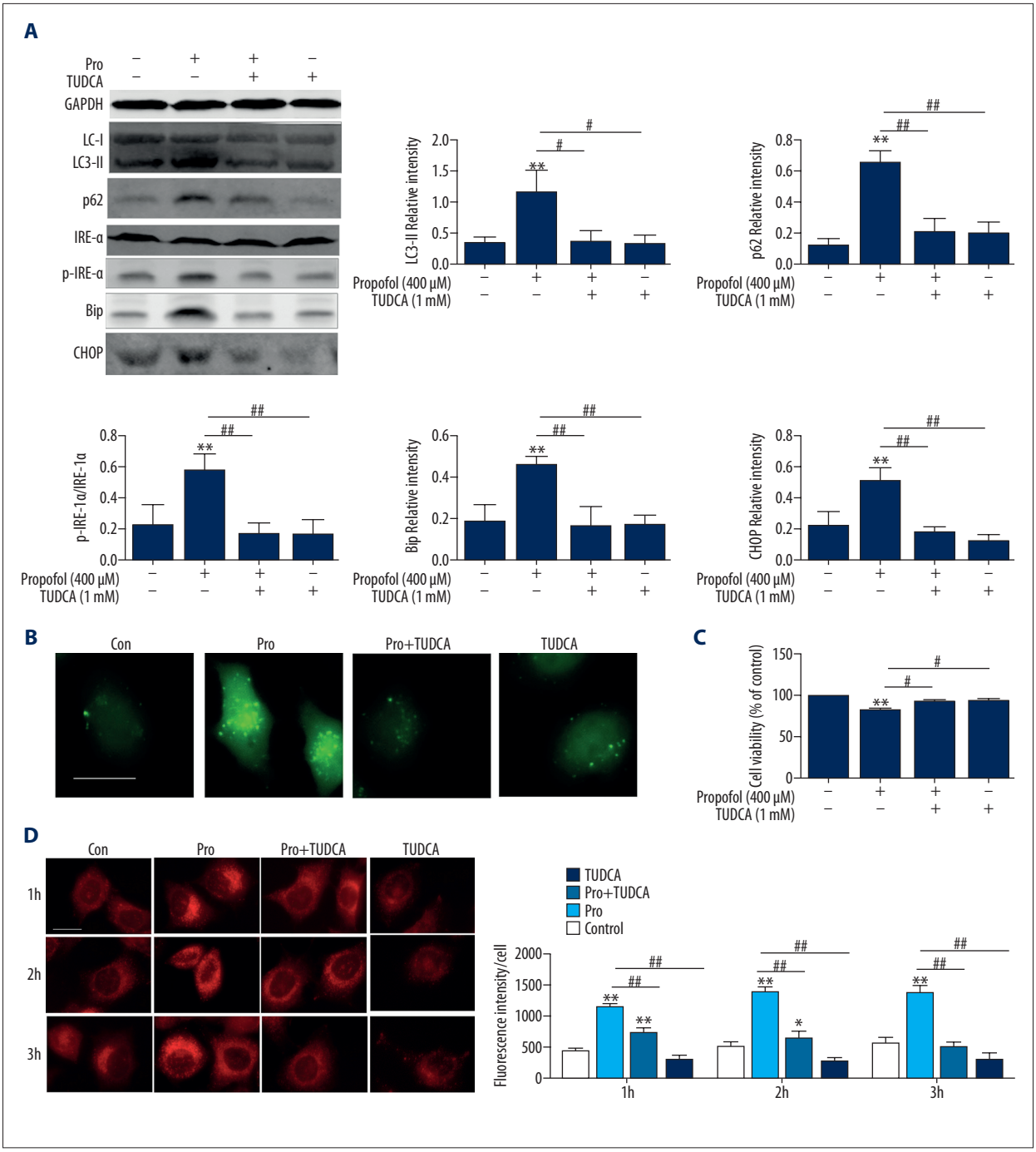

Figure 4. ER stress is involved in propofol-induced autophagy. (**A**) ER stress following propofol treatment was evaluated based on determination of Bip, IRE-1α, phosphorylated (p)-IRE-1α, and CHOP levels using Western blot analysis. LC3 conversion and p62 levels in HeLa cells, as determined by Western blot analysis. (**B**) HeLa cells stably expressing GFP-LC3 were exposed to propofol ([Pro] 400 μM) for 3 h with or without TUDCA (1 mM); untreated cells served as the control (Con). The fluorescence of LC3 punctae was visualized. Treatment with TUDCA in the presence or absence of propofol decreased the number of LC3-positive punctae. Representative images from 4–5 independent experiments are shown. Scale bar=20 μm. (**C**) HeLa cells were co-incubated with 400 μM propofol with or without 1 mM TUDCA for 3 h, and cell viability was determined with CCK-8. (**D**) HeLa cells were treated with 400 μM propofol, TUDCA, or both and intracellular Ca^{2+} was detected using Rhod-2 AM (red fluorescence) for 1 h, 2 h, and 3 h (scale bar=20 μm). Data are expressed as the mean ±S.D, n=3, ** p<0.01 (comparison with control), # p<0.01 (comparison with propofol treatment), ## p<0.01 (comparison between propofol treatment times: 1 h, 2 h, and 3 h).

Indexed in: [Current Contents/Clinical Medicine] [SCI Expanded] [ISI Alerting System] [ISI Journals Master List] [Index Medicus/MEDLINE] [EMBASE/Excerpta Medica] [Chemical Abstracts/CAS]

than in cells treated with propofol and TUDCA. These results suggest that propofol perturbs Ca^{2+} homeostasis, thereby inducing ER stress.

Discussion

This study examined the effects of propofol on HeLa human cervical cancer cells. The major findings of this study were that propofol exerts antitumor effects by impairing autophagic flux, which involves induction of ER stress and regulation of AMPK/mTOR signaling. Propofol has recently been shown to reduce tumor size and weight [26,27]. This was confirmed in our study by the observation that HeLa cell viability was reduced by propofol treatment.

Propofol significantly increased the number of GFP-LC3 fluorescent dots dramatically. Additionally, propofol increased the concentration-dependent conversion of LC3 detected by immunoblotting. p62 binds to LC3 and is selectively degraded through autophagy and is a marker of autophagosome clearance that accumulates when this process is perturbed [7]. We observed an increase in p62 level in HeLa cells following propofol stimulation. Propofol had a weak effect on lysosomal pH, whereas cathepsin B activity and lysosomal abundance were increased. This could be due to the reduced consumption of lysosomes that failed to fuse with autophagosomes. Our results suggest that the observed increase in the levels of autophagic markers resulted from suppression of late autophagy, similar to the effects observed with treatment with CQ. Currently, autophagy inhibitors can be divided into 2 categories: early-stage autophagy inhibitors [28] that mainly block the formation of autophagosomes, and late-stage autophagy inhibitors that exert suppressive effects downstream of autophagosome formation, including inhibition of autophagosome and lysosome fusion or blocking degradation of autolysosomes [29]. Autophagy is another cell death program associated with cancer cell death [30] that serves as a self-protection mechanism for survival under extreme conditions. Additionally, the process of tumor cell metastasis may particularly rely on autophagy. Thus, the roles of autophagy in sustaining or killing cancer cells are complicated. Recently, many autophagy inhibitors have been identified and used in cancer treatment [31]. Inhibition of the autophagic pathway is regarded as a promising new strategy for cancer treatment. Additional research is needed to explore this issue and to clarify whether propofol suppresses tumor cells by impairing autophagic in future experiments using different cell types.

Previous studies have suggested that AMPK is a potential target that regulates various signaling pathways [32]. In addition, AMPK activators can suppress several types of tumors [33]. mTOR is known to play a central role in antitumor activity among the signaling pathways regulated by AMPK [34]. However, the role of mTOR in cancer is complex [35]. mTOR signaling is an important pathway for cell growth and proliferation [36], whereas other research has indicated that mTOR activation inhibits cancer cell proliferation [37]. The positive or negative role of mTOR in tumor growth depends on the complicated environment. Our study indicates that activation of the mTOR signaling pathway contributed to propofol-induced HeLa cell death. Propofol appears to be both an mTOR inhibitor and an AMPK activator. Further studies are underway to investigate the potential use of the AMPK/mTOR pathway as a specific target for therapy in cervical cancer and the sensitivity of mTOR inhibitors to cervical cancer *in vivo*.

Autophagy contributes to apoptosis in several different ways, including enabling membrane blebbing and phosphatidylserine exposure by maintaining ATP levels [38]. Young et al. found that autophagosome formation is involved in the process of apoptosis. Several studies have shown that the activation of AMPK and inhibition of mTOR in addition to autophagy is closely related to apoptosis [39–41]. Nonetheless, the antitumor mechanisms of propofol are complicated. The relationship between propofol-induced autophagy and apoptosis and the underlying mechanisms deserve further investigation. Similarly, several earlier studies demonstrated that the use of autophagy inhibitors targeted against autophagy-associated genes induced apoptosis in various cancer cells [42–45]. These findings raise the possibility of the existence of a potential crosstalk network between autophagy, apoptosis, and feedback, and suggest an attractive strategy for anticancer therapy.

ER stress has been suggested to be a major pathophysiological mechanism in various chronic diseases, including heart disease and cancer [46]. Previous studies have indicated that alteration of the levels of the ER molecular chaperone Bip can inhibit tumor growth *in vivo* [47]. Consistent with this, we found that induction of ER stress resulted in activation of the unfolded protein response (UPR) in HeLa cells treated with propofol, which enhanced cell death by inducing autophagosome accumulation in HeLa cells. An imbalance of Ca^{2+} concentrations between the cytosol and organelles can disrupt autophagy and other Ca^{2+}-dependent cellular processes. Ca^{2+} is also a second messenger in the ER stress response [22], which is linked to dysregulation of Ca^{2+} transport and induction of cell death [48]. When cells experience stimuli such as starvation and disruption of homeostasis, ER stress is activated and Ca^{2+} is transferred from the endoplasmic reticulum to the mitochondria or cytoplasm, subsequently evoking a cytoplasmic Ca^{2+} increase. We also observed that intracellular Ca^{2+} fluorescence was increased in propofol-treated HeLa cells, and this effect was abrogated by TUDCA. Our results suggest that propofol perturbs Ca^{2+} homeostasis not only by causing ER stress but also by enhancing ER stress. Thus, propofol and TUDCA have

Indexed in: [Current Contents/Clinical Medicine] [SCI Expanded] [ISI Alerting System] [ISI Journals Master List] [Index Medicus/MEDLINE] [EMBASE/Excerpta Medica] [Chemical Abstracts/CAS]

opposite effects on the UPR and Ca^{2+} levels in HeLa cells, although the molecular basis of the relationship between these parameters is unclear and warrants further examination. These events are clearly related to autophagy upregulation, but for as yet unknown reasons. Whether propofol-induced autophagy requires Ca^{2+} should be tested in future experiments using different cell types under various stresses.

Conclusions

In conclusion, this study demonstrates for the first time that propofol exerts antitumor effects in HeLa cells by promoting autophagosome accumulation via inhibition of autophagy flux.

Conflicts of interest

None.

References:

1. Miyata T, Kodama T, Honma R et al: Influence of general anesthesia with isoflurane following propofol-induction on natural killer cell cytotoxic activities of peripheral blood lymphocytes in dogs. J Vet Med Sci, 2013; 75(7): 917–21
2. Siddiqui RA, Zerouga M, Wu M et al: Anticancer properties of propofol-docosahexaenoate and propofol-eicosapentaenoate on breast cancer cells. Breast Cancer Res, 2005; 7(5): R645–54
3. Mammoto T, Mukai M, Mammoto A et al: Intravenous anesthetic, propofol inhibits invasion of cancer cells. Cancer Lett, 2002; 184(2): 165–70
4. Kashiwagi A, Hosokawa S, Maeyama Y et al: Anesthesia with disuse leads to autophagy up-regulation in the skeletal muscle. Anesthesiology, 2015; 122(5): 1075–83
5. Al-Ejeh F, Kumar R, Wiegmans A et al: Harnessing the complexity of DNA-damage response pathways to improve cancer treatment outcomes. Oncogene, 2010; 29(46): 6085–98
6. Klionsky DJ, Abdelmohsen K, Abe A et al: Guidelines for the use and interpretation of assays for monitoring autophagy (3rd edition). Autophagy, 2016; 12(1): 1–222
7. Zhou J, Hu SE, Tan SH et al: Andrographolide sensitizes cisplatin-induced apoptosis via suppression of autophagosome-lysosome fusion in human cancer cells. Autophagy, 2012; 8(3): 338–49
8. Chang CP, Yang MC, Lei HY: Concanavalin A/IFN-gamma triggers autophagy-related necrotic hepatocyte death through IRGM1-mediated lysosomal membrane disruption. PLoS One, 2011; 6(12): e28323
9. Kosta A, Roisin-Bouffay C, Luciani MF et al: Autophagy gene disruption reveals a non-vacuolar cell death pathway in Dictyostelium. J Biol Chem, 2004; 279(46): 48404–9
10. Ma X, Liu H, Foyil SR et al: Impaired autophagosome clearance contributes to cardiomyocyte death in ischemia/reperfusion injury. Circulation, 2012; 125(25): 3170–81
11. Cook KL, Clarke PA, Parmar J et al: Knockdown of estrogen receptor-alpha induces autophagy and inhibits antiestrogen-mediated unfolded protein response activation, promoting ROS-induced breast cancer cell death. FASEB J, 2014; 28(9): 3891–905
12. Cao SS, Kaufman RJ: Unfolded protein response. Curr Biol, 2012; 22(16): R622–26
13. Shi H, Magaye R, Castranova V, Zhao J: Titanium dioxide nanoparticles: A review of current toxicological data. Part Fibre Toxicol, 2013; 10: 15
14. Ren G, Zhou Y, Liang G et al: General anesthetics regulate autophagy via modulating the inositol 1,4,5-trisphosphate receptor: Implications for dual effects of cytoprotection and cytotoxicity. Sci Rep, 2017; 7(1): 12378
15. Loetchutinat C, Priebe W, Garnier-Suillerot A: Drug sequestration in cytoplasmic organelles does not contribute to the diminished sensitivity of anthracyclines in multidrug resistant K562 cells. Eur J Biochem, 2001; 268(16): 4459–67
16. Gonzalez P, Mader I, Tchoghandjian A et al: Impairment of lysosomal integrity by B10, a glycosylated derivative of betulinic acid, leads to lysosomal cell death and converts autophagy into a detrimental process. Cell Death Differ, 2012; 19(8): 1337–46
17. Ma X, Godar RJ, Liu H, Diwan A: Enhancing lysosome biogenesis attenuates BNIP3-induced cardiomyocyte death. Autophagy, 2012; 8(3): 297–309
18. Yue W, Hamai A, Tonelli G et al: Inhibition of the autophagic flux by salinomycin in breast cancer stem-like/progenitor cells interferes with their maintenance. Autophagy, 2013; 9(5): 714–29
19. Sheen JH, Zoncu R, Kim D, Sabatini DM: Defective regulation of autophagy upon leucine deprivation reveals a targetable liability of human melanoma cells *in vitro* and *in vivo*. Cancer Cell, 2011; 19(5): 613–28
20. Wang X, Wang Z, Yao Y et al: Essential role of ERK activation in neurite outgrowth induced by alpha-lipoic acid. Biochim Biophys Acta, 2011; 1813(5): 827–38
21. Saiki S, Sasazawa Y, Imamichi Y et al: Caffeine induces apoptosis by enhancement of autophagy via PI3K/Akt/mTOR/p70S6K inhibition. Autophagy, 2011; 7(2): 176–87
22. Yoon YH, Cho KS, Hwang JJ et al: Induction of lysosomal dilatation, arrested autophagy, and cell death by chloroquine in cultured ARPE-19 cells. Invest Ophthalmol Vis Sci, 2010; 51(11): 6030–37
23. Shinojima N, Yokoyama T, Kondo Y, Kondo S: Roles of the Akt/mTOR/p70S6K and ERK1/2 signaling pathways in curcumin-induced autophagy. Autophagy, 2007; 3(6): 635–37
24. Cherla RP, Lee SY, Mulder RA et al: Shiga toxin 1-induced proinflammatory cytokine production is regulated by the phosphatidylinositol 3-kinase/Akt/mammalian target of rapamycin signaling pathway. Infect Immun, 2009; 77(9): 3919–31
25. Qiao D, Meyer K, Friedl A: Glypican 1 stimulates S phase entry and DNA replication in human glioma cells and normal astrocytes. Mol Cell Biol, 2013; 33(22): 4408–21
26. Cui WY, Liu Y et al: Propofol induces endoplasmic reticulum (ER) stress and apoptosis in lung cancer cell H460. Tumour Biol, 2014; 35(6): 5213–17
27. Zhang J, Shan WF, Jin TT et al: Propofol exerts anti-hepatocellular carcinoma by microvesicle-mediated transfer of miR-142-3p from macrophage to cancer cells. J Transl Med, 2014; 12: 279
28. Blommaart EF, Krause U, Schellens JP et al: The phosphatidylinositol 3-kinase inhibitors wortmannin and LY294002 inhibit autophagy in isolated rat hepatocytes. Eur J Biochem, 1997; 243(1–2): 240–46
29. Yang YP, Hu LF, Zheng HF et al: Application and interpretation of current autophagy inhibitors and activators. Acta Pharmacol Sin, 2013; 34(5): 625–35
30. Yang ZJ, Chee CE, Huang S, Sinicrope FA: The role of autophagy in cancer: Therapeutic implications. Mol Cancer Ther, 2011; 10(9): 1533–41
31. Zhao X, Fang Y, Yang Y et al: Elaiophylin, a novel autophagy inhibitor, exerts antitumor activity as a single agent in ovarian cancer cells. Autophagy, 2015; 11(10): 1849–63
32. Karnevi E, Said K, Andersson R, Rosendahl AH: Metformin-mediated growth inhibition involves suppression of the IGF-I receptor signalling pathway in human pancreatic cancer cells. BMC Cancer, 2013; 13: 235
33. Adekola K, Popat U, Ciurea SO: An update on allogeneic hematopoietic progenitor cell transplantation for myeloproliferative neoplasms in the era of tyrosine kinase inhibitors. Bone Marrow Transplant, 2014; 49(11): 1352–59
34. Zheng QY, Jin FS, Yao C et al: Ursolic acid-induced AMP-activated protein kinase (AMPK) activation contributes to growth inhibition and apoptosis in human bladder cancer T24 cells. Biochem Biophys Res Commun, 2012; 419(4): 741–47
35. Castedo M, Ferri KF, Kroemer G: Mammalian target of rapamycin (mTOR): Pro- and anti-apoptotic. Cell Death Differ, 2002; 9(2): 99–100
36. Zoncu R, Efeyan A, Sabatini DM: mTOR: From growth signal integration to cancer, diabetes and ageing. Nat Rev Mol Cell Biol, 2011; 12(1): 21–35
37. Lee JY, Nakada D, Yilmaz OH et al: mTOR activation induces tumor suppressors that inhibit leukemogenesis and deplete hematopoietic stem cells after Pten deletion. Cell Stem Cell, 2010; 7(5): 593–605

Indexed in: [Current Contents/Clinical Medicine] [SCI Expanded] [ISI Alerting System] [ISI Journals Master List] [Index Medicus/MEDLINE] [EMBASE/Excerpta Medica] [Chemical Abstracts/CAS]

38. Bovellan M, Fritzsche M, Stevens C, Charras G: Death-associated protein kinase (DAPK) and signal transduction: blebbing in programmed cell death. FEBS J, 2010; 277(1): 58–65
39. Jang JE, Eom JI, Jeung HK et al: AMPK-ULK1-mediated autophagy confers resistance to BET inhibitor JQ1 in acute myeloid leukemia stem cells. Clin Cancer Res, 2017; 23(11): 2781–94
40. Liu X, Hu X, Kuang Y et al: BCLB, methylated in hepatocellular carcinoma, is a starvation stress sensor that induces apoptosis and autophagy through the AMPK-mTOR signaling cascade. Cancer Lett, 2017; 395: 63–71
41. Song X, Kim SY, Zhang L et al: Role of AMP-activated protein kinase in cross-talk between apoptosis and autophagy in human colon cancer. Cell Death Dis, 2014; 5: e1504
42. Boya P, Gonzalez-Polo RA, Casares N et al: Inhibition of macroautophagy triggers apoptosis. Mol Cell Biol, 2005; 25(3): 1025–40
43. Kanzawa T, Germano IM, Komata T et al: Role of autophagy in temozolomide-induced cytotoxicity for malignant glioma cells. Cell Death Differ, 2004; 11(4): 448–57
44. Kanzawa T, Kondo Y, Ito H et al: Induction of autophagic cell death in malignant glioma cells by arsenic trioxide. Cancer Res, 2003; 63(9): 2103–8
45. Paglin S, Hollister T, Delohery T et al: A novel response of cancer cells to radiation involves autophagy and formation of acidic vesicles. Cancer Res, 2001; 61(2): 439–44
46. Kim I, Xu W, Reed JC: Cell death and endoplasmic reticulum stress: Disease relevance and therapeutic opportunities. Nat Rev Drug Discov, 2008; 7(12): 1013–30
47. Moenner M, Pluquet O, Bouchecareilh M, Chevet E: Integrated endoplasmic reticulum stress responses in cancer. Cancer Res, 2007; 67(22): 10631–34
48. Hung YH, Chen LM, Yang JY, Yang WY: Spatiotemporally controlled induction of autophagy-mediated lysosome turnover. Nat Commun, 2013; 4: 2111

Indexed in: [Current Contents/Clinical Medicine] [SCI Expanded] [ISI Alerting System] [ISI Journals Master List] [Index Medicus/MEDLINE] [EMBASE/Excerpta Medica] [Chemical Abstracts/CAS]